A Chemical Definition of the Boundary of the Antarctic Ozone Hole

M. H. PROFFITT,[1,2] J. A. POWELL,[1,2] A. F. TUCK,[1] D. W. FAHEY,[1] K. K. KELLY,[1]
A. J. KRUEGER,[3] M. R. SCHOEBERL,[3] B. L. GARY,[4] J. J. MARGITAN,[4]
K. R. CHAN,[5] M. LOEWENSTEIN,[5] AND J. R. PODOLSKE[5]

A campaign utilizing an ER-2 high-altitude aircraft and a DC-8 aircraft, both fitted with state-of-the-art instrumentation to study the Antarctic ozone hole, was conducted out of Punta Arenas, Chile, from August 17 through September 22, 1987. Data indicated a chemically perturbed region roughly coincident with the Antarctic polar vortex and with the region of large temporal decrease of ozone that is usually referred to as the Antarctic ozone hole. A rapid rise in ClO was observed as the ER-2 proceeded into the ozone hole at about 18 km altitude, and it is this feature that is used to define the boundary of the chemically perturbed region as that latitude along the flight track where ClO reaches 130 parts per trillion by volume (pptv). In situ data taken simultaneously aboard the ER-2, as well as Total Ozone Mapping Spectrometer (TOMS) satellite ozone data along the flight tracks, are analyzed at fixed positions relative to this boundary and are presented as averages over the duration of the mission. These analyses indicate a narrow transition zone at the boundary for the chemically active species ClO, O_3, NO_y, and NO. A somewhat wider transition zone for the chemical species N_2O and H_2O and for the meteorological parameters of temperature, wind speed, and potential vorticity is also seen, indicating the dynamical character of the chemically defined boundary. TOMS column values of about 260 Dobson units (DU) generally persisted at the boundary during this period. One-month temporal trends of the in situ data both inside and outside this boundary are also presented. Interpretations of these analyses are offered that are consistent with ongoing diabatic cooling, accompanying advective poleward transport across the boundary. These data strongly implicate man's release of chlorine into the atmosphere as a necessary ingredient in the formation of the Antarctic ozone hole.

INTRODUCTION

During the 1987 Airborne Antarctic Ozone Experiment (AAOE), an ER-2 aircraft made 12 flights out of Punta Arenas, Chile (53°S, 71°W), into the Antarctic polar vortex. The aircraft carried fast-response instruments for in situ measurements of many trace species, including ozone (O_3), chlorine monoxide (ClO), bromine monoxide (BrO), the sum of the reactive nitrogen oxide species (abbreviated as NO_y and including NO, NO_2, NO_3, HNO_3, N_2O_5, and $ClONO_2$), nitric oxide (NO), total water content (H_2O, gas and particles), and nitrous oxide (N_2O). Grab samples of long-lived tracers were also taken, and a scanning microwave radiometer measured temperatures above and below the aircraft. In situ measurements of condensation nuclei and particle size distributions and the meteorological parameters of temperature, pressure, and wind speed were also made. Most of these flights were made poleward to 72°S at a high altitude and constant potential temperature, followed by a descent to a lower altitude and a return leg, again at a high altitude and constant potential temperature. A potential temperature surface of 425 ± 10 K (about 17.5 km altitude) was chosen for 12 of the flight legs, and 450 ± 10 K (about 19 km altitude) for six of the flight legs. Of the remaining six legs of the 12 flights, one was flown in part on each of these two surfaces, but the others were flown without regard for potential

[1]Aeronomy Laboratory, Environmental Research Laboratories, NOAA, Boulder, Colorado.
[2]Also at Cooperative Institute for Research in Environmental Sciences, University of Colorado, Boulder.
[3]NASA Goddard Space Flight Center, Greenbelt, Maryland.
[4]Jet Propulsion Laboratory, University of California, Pasadena.
[5]NASA Ames Research Center, Moffett Field, California.

temperature. Only the 10 flights from August 23 through September 22 are included in our analysis. The two earlier flights (August 17 and August 18) are not included, since not all instruments were fully operational. These flights did not include the midflight descent, nor did they penetrate as far south as the other 10 flights. All flights were approximately 6 hours in duration and attained their southernmost point at midday. (See Tuck [this issue] and Tuck et al. [this issue] for a detailed overview of the mission and its goals. For a short discussion of the use of potential temperature in the flight planning also see Proffitt et al. [1989a].)

The in situ measurements taken from the ER-2 clearly trace the development of the ozone hole during the 10 flights analyzed [Tuck, this issue]. Although the aircraft covered a limited range of latitude and longitude relative to the size of the ozone hole and was never within the region of minimum column ozone (as indicated by the Total Ozone Mapping Spectrometer (TOMS) satellite images), the measured values of ClO, NO, NO_y, and H_2O indicated a chemically perturbed region roughly coincident with latitudes of large temporal ozone decrease. In particular, within the chemically perturbed region, ClO levels were observed to be more than 100 times those expected from mid-latitude measurements, indicating very disturbed chlorine chemistry [Brune et al., 1989]. In addition, the values for NO, NO_y, and H_2O indicated that the air was denitrified and dehydrated. Current chemical models used to explain the observed decreases of ozone within the chemically perturbed region require low values of NO_2 to restrict its combination with ClO and BrO to form the unreactive reservoir species $ClONO_2$ and $BrONO_2$ [Molina and Molina, 1987; McElroy et al., 1986; Solomon et al., 1986]. The low measured values of NO and NO_y indirectly reflect the low NO_2 required by the models, and the low H_2O values indicate a possible mechanism for removal of NO_y via incorporation of HNO_3 within water
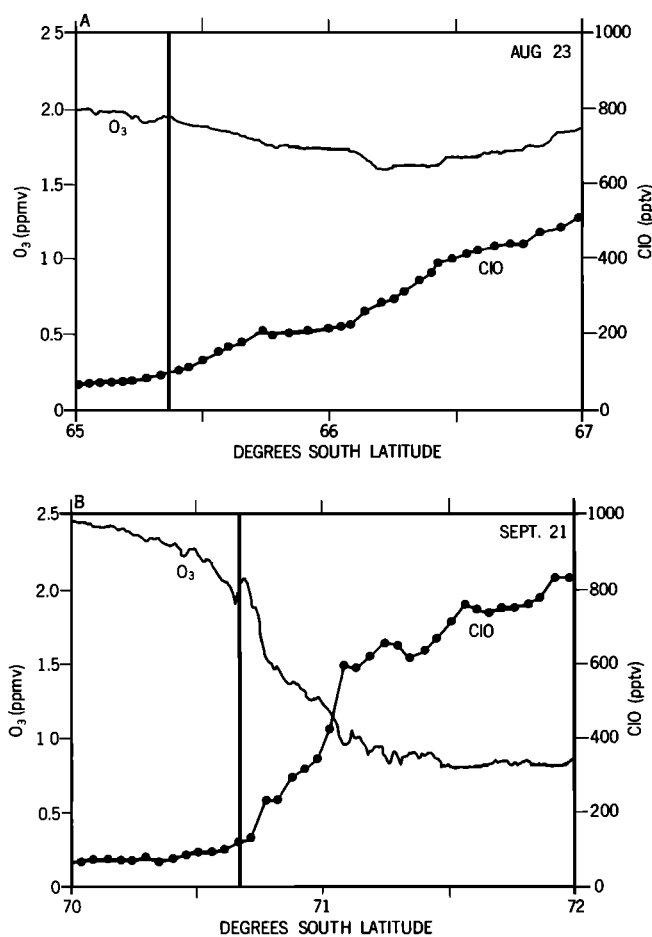
Fig. 1. Ozone and chlorine monoxide when crossing the boundary of the chemically perturbed region (a) on August 23 and (b) on September 21. The ordinate is latitude and the heavy vertical lines indicate the boundary of the chemically perturbed region.

particles, followed by removal through sedimentation [Fahey et al., this issue]. This removal process (dehydration and denitrification by cooling, followed by sedimentation of particles) was not directly observed during the mission; however, meteorological data indicate that temperatures over parts of Antarctica were cold enough to continue to dehydrate and produce the low water mixing ratios observed until about mid-September [Kelly et al., this issue]. Discussions of the implications of this perturbed chemistry and the chemical destruction of ozone by chlorine can be found in other AAOE papers [Rodriguez et al., 1989; Ko et al., 1989; Anderson et al., this issue].

As the mission progressed, a striking negative correlation developed between the measured values of O_3 and ClO in the narrow transition zone from inside to outside the chemically perturbed region [Murphy et al., this issue; Anderson et al., this issue]. For example, see Figure 1a, where early in the mission, at a potential temperature of about 425 K, ClO levels were a factor of 10 higher inside the region, and ozone shows a decrease of about 15% across the boundary. On that flight the aircraft ascended to a higher potential temperature between 66° and 67°S latitude, with the expected increase in ozone and ClO with altitude, making isentropic comparison beyond this point impossible. One month later (Figure 1b), we observe that within 1° of latitude, O_3 decreased by more

than 60% and ClO again increased by a factor of 10. The latitude locating this rapid increase of ClO was observed to change by more than 5° within 1 day. These variations in location of the vortex boundary are of the same magnitude as the penetration of the ER-2 into the vortex (a few degrees to 10°), making flight-to-flight comparison of data at fixed latitudes difficult to interpret. By referencing each flight leg to the latitude of this abrupt transition, we eliminate this difficulty.

Although other trace constituents also showed large changes going into the chemically perturbed region, the largest gradient with latitude was in ClO. Here our intent is to present a viable definition for the boundary of the chemically perturbed region, using ClO values to identify that boundary, and other ER-2 measurements to support its validity. This boundary can then serve as a reference point for comparing the various trace species and dynamical parameters measured, for determining their averaged characteristic latitude plots (averaged over the duration of the mission and latitude relative to the boundary), for calculating temporal trends inside and outside the boundary, and for comparing their spatial distributions. Such analyses and elementary interpretation of these analyses are presented here; more detailed analyses are presented elsewhere [Fahey et al., 1989; Proffitt et al., 1989a, b; Hartmann et al., this issue]. Our analyses will be primarily concerned with accurately locating the boundary of the ozone hole, as defined by large temporal decreases in ozone, investigating the location of the high ClO values relative to those large ozone losses, and investigating the atmospheric dynamics within about 5° in latitude either side of the boundary.

DEFINITION OF BOUNDARY OF CHEMICALLY PERTURBED REGION

As just discussed, large increases in ClO were observed in less than 1° of latitude, as the aircraft flew southward. The range of values along the flight legs was from a minimum of about 10 parts per trillion by volume (pptv), when about 10°–12° of latitude north of the large ClO increases, to a maximum of about 1200 pptv late in the mission and at 450 K and 72°S. The largest latitude gradient generally occurred between 100 and 200 pptv. On the basis of these observations, a value of 130 pptv was chosen to define the boundary, a value about 10 times more than the lowest values observed and about 10 times less than the highest values observed. Other choices for the boundary ranging from 100 to 200 pptv would be equally appropriate and would change the position of the boundary only a few tens of minutes of latitude.

With this in mind, we formally define this boundary as follows. Along any flight leg, the boundary of the chemically perturbed region is the northmost latitude, such that the mixing ratio of ClO is greater than 130 pptv at all positions on that flight leg south of that latitude. For most of the flight legs this is equivalent to the simplified definition obtained by deleting the words "at all positions on that flight leg south of that latitude"; however, on a few of the flight legs the ClO value reaches 130 pptv but drops to lower values to the south before attaining and remaining above the 130 pptv level, as is required by the definition. It should be noted that the boundary is defined identically for both flight levels, although ClO mixing ratios are altitude-dependent. An altitude-dependent definition would be necessary to cover the

TABLE 1.   Values at Boundary of Chemically Perturbed Region

	Boundary Latitude	Potential Temperature, °K	TOMS Column Ozone, DU	Potential Vorticity, K Pa^{-1} s^{-1}	Latitude of Water Edge
Aug. 23, 1987	65°20'	421	322	-2.57E-5	66°0'
	66°10'	454	308	-4.22E-5	66°30'
Aug. 28, 1987	69°0'	425	260	-2.25E-5	none
	69°0'	419	260	-2.09E-5	69°20'
Aug. 30, 1987	64°40'	423	243	-2.50E-5	68°10'
	65°20'	424	241	-2.19E-5	66°30'
Sept. 2, 1987	62°30'	432	274	-2.80E-5	62°20'
	62°10'	434	278	-2.85E-5	62°30'
Sept. 4, 1987	64°20'	422	244	-2.32E-5	65°0'
	65°20'	424	238	-2.46E-5	65°20'
Sept. 9, 1987	59°30'	446	272	-2.73E-5	58°0'
	60°20'	420	261	-2.69E-5	60°0'
Sept. 16, 1987	67°30'	453	252	-4.01E-5	67°20'
	67°50'	424	249	-2.95E-5	67°30'
Sept. 20, 1987	68°10'	447	255	-4.33E-5	67°30'
	68°0'	457	257	-4.79E-5	67°40'
Sept. 21, 1987	70°40'	453	234	none	70°30'
	69°40'	428	259	-2.82E-5	69°10'
Sept. 22, 1987	64°30'	455	266	-3.79E-5	63°50'
	64°50'	430	265	-2.76E-5	64°30'
Averages	65°44' ± 3°6'		262 ± 22		65°40'
TOMS average excluding August 23			256 ± 13		

Latitudes stated for boundary are within 10 minutes of latitude and the potential vorticity is calculated from ER-2 data alone. Read −2.57E−5 as −2.57 × 10^{-5}.

entire range of known ozone decrease of from 12 to 20 km [*Hoffmann et al.*, 1987], but it is not needed for the limited range used here.

In Table 1 we chronologically list the latitudes of the boundary of the chemically perturbed region for all of the ER-2 flight legs from August 23 through September 22. Over the course of the mission, the range in latitude of the boundary is 11°. These latitude changes do not appear systematic, but they do reflect the movement of the polar jet. For comparison purposes we have listed the "dehydration edge," as described by *Kelly et al.* [this issue]. Except for 2 days, the boundary and the edge agree within 1° of latitude. We have also included the TOMS ozone column measurements at the point along the ER-2 flight track corresponding to the boundary [*Krueger et al.*, 1988], along with the mission averages and sample standard deviations. Excluding the values on August 23, the total ozone averaged 256 Dobson units (DU) (1 DU = 1 milli-atm-cm ozone), with a sample standard deviation of 13 DU. The data set on August 23 is anomalous (more than 300 DU), possibly because of the unusual meteorological conditions on that day. As discussed by *Proffitt et al.* [1989b], conditions outside the boundary were influenced by the subtropical jet becoming coincident with the polar jet on that date, thereby bringing air from much lower latitudes into that region. ER-2 data taken on this date is considered as a special case and is discussed later. In addition, the highest values of ozone observed in situ during the mission were seen on that day near the boundary at the 450 K flight level. This is consistent with the high column ozone measured at the boundary on that day. The potential temperature and potential vorticity values along the flight legs at the boundary are included in Table 1. Details on potential vorticity calculations can be found elsewhere [*Hartmann et al.*, this issue].

Figures 2a and 2b demonstrate the effect of this definition by averaging the ClO data on the 425 K flight legs in two different ways. The 425 K data is first averaged over all 10 flights by latitude (Figure 2a) and then it is averaged relative to the boundary (Figure 2b). Data from 450 K flight legs relative to the boundary are included as Figure 2c. In all cases the data were also averaged over 1° latitude bins. The vertical bars indicate the sample standard deviations of the N 1° averages, where N is given directly below the bars. (Throughout this paper standard deviations are given as sample standard deviations, rather than standard deviations of the mean. The sample standard deviation indicates the scatter in the N measurements, rather than the uncertainty of the average, which is obtained by dividing our result by N − 1). The steep gradient with latitude is faithfully reproduced in Figures 2b and 2c, but not in Figure 2a. Bearing this in mind, one can see that from 60° to 70°S latitude, statistical studies involving column ozone measurements at fixed latitudes will be sampling both inside and outside the chemically perturbed region and will not accurately reflect its sharp boundary.

Table 2 presents 1-month temporal trends with respect to the boundary of various chemical and meteorological parameters, determined by linear least squares fits to the data from August 23 through September 22. Also indicated in Table 2 are the standard deviations of the residuals, expressed as percent of the value at the midpoint of the fit and indicated as the error limits. The number of data points determining the linear fits for ClO, O_3, H_2O, N_2O, and potential temperature is given within parenthesis. The number of data points determining the NO_y, potential vorticity, wind speed, and temperature temporal trends is slightly less, as discussed in the next section of this paper. A trend less than or equal to its residual is not considered to be significantly different from
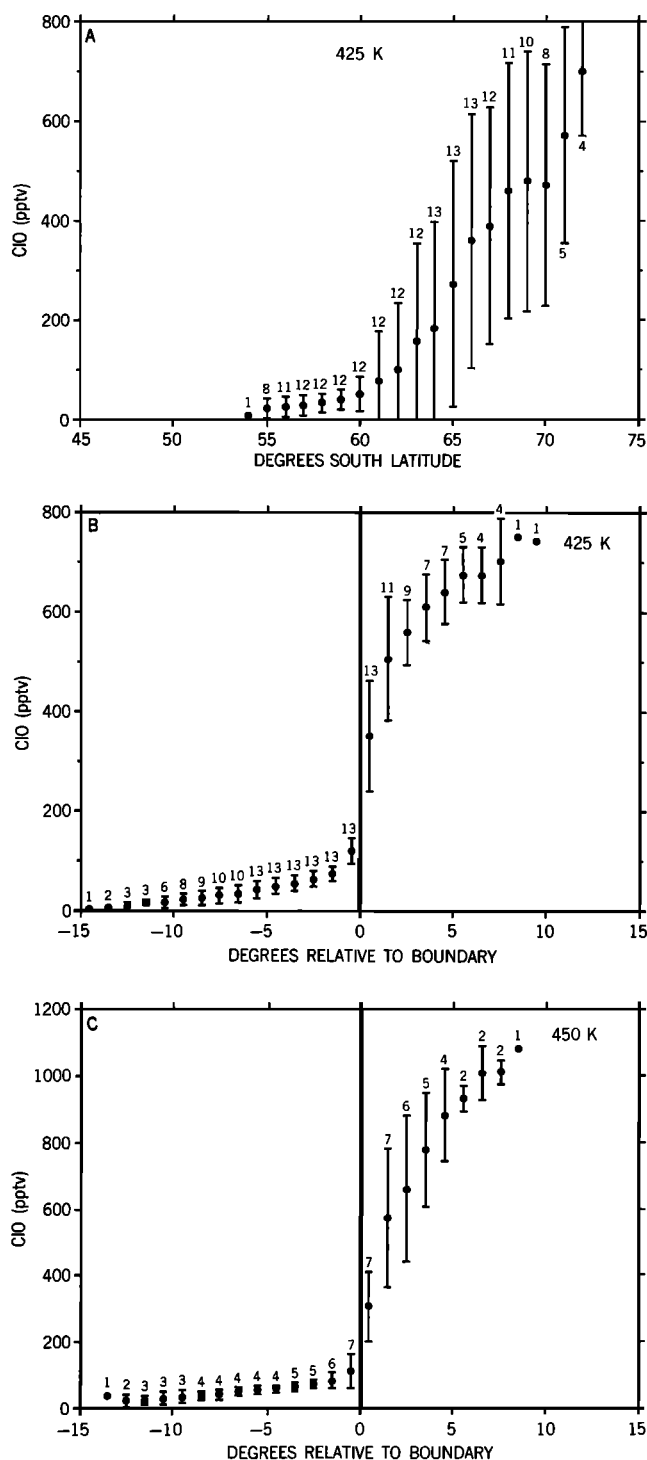
Fig. 2. (a) Plot of averaged ClO versus latitude for the 425 K flight level. Data are averaged over 1° latitude intervals and include all 425 K flight legs, from August 23 through September 22. (b) As in Figure 2a, except averages are made with respect to the boundary of the chemically perturbed region. (c) As in Figure 2b, except for all 450 K flight legs.

zero, the residual being used as an indication of the uncertainty of the temporal trend. In all cases we have included temporal trends only if there are data available from both the first week and the last week of the 1-month period.

The temporal trends in ClO are given in the second column of Table 2. From those trends that are significantly different

from zero, we again see that our choice of 130 pptv of ClO for the boundary is a reasonable choice for the division between two very different regions of the Antarctic stratosphere. At 425 K we find that within the boundary there are large increases in ClO of from 31% to 107% over the 1-month period, but only decreases are seen outside. At 450 K we see the trends are not significantly different from zero for the first 4° inside and that their residuals are about 30%, indicating that temporal trends are less than those at 425 K. Outside the boundary we again see a large decrease at 450 K, even larger than that observed at 425 K. In the next section of this paper we will offer a few broad stroke interpretations for each of the species, immediately following the general description of the data for that species. Therefore we begin that practice here with ClO.

The upward temporal trend in ClO inside at 425 K is consistent with the decreases seen in NO_y, as discussed earlier. However, the trends in ClO inside and at 450 K do not seem consistent with the observed decreases in NO_y at that level. The temporal trends in H_2O at both levels indicate a resupply of air across the boundary, which complicates a simple interpretation of the ClO trends. For a detailed account of evidence for such a resupply of air across the boundary via diabatic cooling and poleward transport, see *Proffitt et al.* [1989b]. We do not offer an explanation for the temporal decreases seen outside the boundary, except to mention that the residuals are, in most cases, nearly as large as the trends themselves, indicating less confidence than we have for the increasing trends.

AVERAGED IN SITU MEASUREMENTS AND TEMPORAL TRENDS WITH RESPECT TO THE BOUNDARY

In the previous section we discussed the temporally averaged ClO measurements with respect to the boundary along with the ClO temporal trends. We also demonstrated that the boundary, as defined, accurately locates the steep latitudinal gradient in ClO and is useful for interpreting temporal trends of in situ data. Other species have been analyzed with respect to the boundary elsewhere, and some of those species will also be presented here. For example, Table 2 includes temporal trends of O_3 and N_2O that are presented elsewhere in more detail and in a different context than presented here. We will briefly discuss each of the species listed in Table 2, along with their temporally averaged plots, offering a few simple interpretations of these data, as we did for ClO.

Before we start the discussion of the other species, we need to make a few remarks concerning the first flight of our analysis, on August 23. We have mentioned earlier that meteorologically, August 23 was an unusual date, when the subtropical jet became coincident with the polar jet. Furthermore, it was a flight where no attempt was made to fly on constant potential temperature surfaces. Therefore trend analysis that includes this date must be done with care. *Proffitt et al.* [1989b] make a very detailed analysis of N_2O data, especially regarding the August 23 data. It was determined that where there were data on August 23 within the potential temperature ranges of 425 K ±10 and 450 K ±10, the temporal trends for N_2O that included these data were generally consistent with a more detailed trend analysis, where potential temperature variations were considered. On the basis of the N_2O data, we conclude that although there

TABLE 2. One-Month Temporal Trends, From August 23 Through September 22, 1987

Degrees Relative to Boundary (425 ± 10 K)	ClO, %	O₃, %	NOy, %	H₂O, %	N₂O, %	PV, %	WS, %	Temperature, %	Potential Temperature and Average
Outside the Boundary									
−5 (13)	−27 ± 34	−7 ± 9	−8 ± 20	+19 ± 3	+12 ± 10	−14 ± 7	+37 ± 13	+2.3 ± 1.1	+1.5 ± 1.0% 423K
−4 (13)	−27 ± 31	−15 ± 6	−12 ± 12	+14 ± 3	+6 ± 8	−5 ± 14	+39 ± 11	+1.8 ± 1.0	+0.9 ± 1.0% 424K
−3 (13)	−26 ± 23	−16 ± 8	−10 ± 12	+11 ± 3	+7 ± 9	−8 ± 6	+56 ± 9	+2.2 ± 1.4	+0.6 ± 0.9% 423K
−2 (13)	−30 ± 19	+4 ± 5	−7 ± 14	+18 ± 3	+4 ± 7	−15 ± 5	+66 ± 10	+3.0 ± 1.3	+1.1 ± 0.7% 424K
−1 (13)	−14 ± 21	+4 ± 7	−2 ± 7	+18 ± 2	0 ± 7	−26 ± 7	+86 ± 11	+2.9 ± 1.2	+1.6 ± 1.0% 424K
Inside the Boundary									
+1 (13)	+107 ± 22	−49 ± 7	−45 ± 16	+3 ± 6	−15 ± 5	−30 ± 9	+92 ± 10	+2.7 ± 1.3	+0.3 ± 1.2% 425K
+2 (11)	+101 ± 13	−61 ± 5	−51 ± 26	−13 ± 9	−10 ± 7	−27 ± 9	+65 ± 11	+4.0 ± 1.3	−1.1 ± 1.1% 426K
+3 (9)	+43 ± 8	−62 ± 4	−51 ± 24	−31 ± 9	−25 ± 6	−27 ± 8	+73 ± 7	+4.9 ± 1.1	+0.0 ± 1.3% 426K
+4 (7)	+49 ± 3	−46 ± 6	−83 ± 56	−42 ± 14	−27 ± 6	−26 ± 7	+96 ± 7	+5.0 ± 0.8	+0.7 ± 1.0% 424K
+5 (7)	+31 ± 7	−51 ± 7	−67 ± 27	−29 ± 15	−13 ± 2	−8 ± 8	+40 ± 7	+3.2 ± 1.0	−1.5 ± 0.3% 422K

Degrees Relative to the Boundary (450 ± 10 K)	ClO, %	O₃, %	NOy, %	H₂O, %	N₂O, %	Potential Temperature and Average
Outside the Boundary						
−1 (7)	−53 ± 29	−16 ± 15		+16 ± 6	+9 ± 3	+1.5 ± 1.0% 453 K
Inside the Boundary						
+1 (7)	−30 ± 32	−44 ± 13	−44 ± 22	0 ± 6	−6 ± 9	+0.3 ± 0.8% 451 K
+2 (7)	−25 ± 36	−46 ± 10	−48 ± 21	+11 ± 8	−7 ± 6	+2.7 ± 0.9% 450 K
+3 (6)	−6 ± 37	−50 ± 8	−44 ± 19	+12 ± 9	−7 ± 7	+2.7 ± 0.7% 448 K
+4 (5)	+7 ± 26	−56 ± 11	−40 ± 9	−14 ± 15	−6 ± 5	+1.4 ± 0.7% 446 K
+5 (4)	+29 ± 14	−62 ± 2		+24 ± 14	−2 ± 5	+2.8 ± 1.0% 444 K

Temporal trends indicate linear fit to temporal data during a 1-month period and error limits are the residuals expressed as percent of the value at the midpoint of the fit. The data are averaged beginning at the position given in the table (degrees relative to boundary) and ending 1° of latitude nearer the boundary. The numbers in parenthesis are the number of data points used in the trend analysis, except for NOy, potential verticity (PV), wind speed (WS), and temperatures, as discussed in text. The average potential temperature is also given.

was a significant meteorological anomaly on this date that is reflected in the wind and temperature data, there was not substantial replacement of air near the boundary at these potential temperatures. Therefore we could find no reason to exclude that date from the analyses of the in situ trace species. We have excluded August 23 data from the trend analysis only for temperature and wind speed, the derived meteorological quantity of potential vorticity, and for the averaged data plot of TOMS column ozone. All other averaged plots and trend analysis include data from that date. We feel this is the most consistent way to present the data, thereby eliminating undue or arbitrary deletions, although similiar results would be obtained by further deletions from the August 23 data. The potential temperature data clearly must include the data from August 23, since the intent here is to show how well we achieve flying on the constant potential temperature surfaces.

A significant test of the definition of the boundary and of the possible role of chlorine in the destruction of ozone can be achieved by considering the O₃ data referenced to the boundary. For if the temporal decreases in O₃ are not precisely collocated with the high ClO levels, it would cast doubt on whether chlorine plays a dominant role in the formation of the ozone hole. However, we can see from Table 2 that in the region 1° of latitude inside the boundary, ozone decreased almost 50% in 1 month, but in the region 1° of latitude outside the boundary, ozone showed no significant trend at 425 K and a marginally significant downward trend at 450 K. In this sense the boundary of the chemically perturbed region is coincident with the boundary of the

ozone hole to within 1° of latitude. This means that the steep horizontal gradient in ClO is coincident with the region of large temporal decrease of ozone. Although this does not prove that chlorine is the primary cause of the ozone hole, this narrow anticorrelation, accompanied by ClO levels sufficient to produce large ozone losses within the boundary, is the strongest evidence from the mission indicating the role of chlorine. Of course, this anticorrelation is also evident in the averaged data plot (Figure 3). Since this is temporally averaged data over the 1-month period, the averages include the ozone levels from August, before the ozone hole was highly developed.

Here we also include a brief look at the TOMS satellite ozone measurements that were made coincident with the ER-2 flight tracks [Krueger et al., 1988]. Since TOMS measures total column ozone and since the satellite measurements are spatially and temporally averaged, we do not expect as sharp a decrease at the boundary as with the in situ measurements of ozone. Figure 4 presents the column measurements that are comparable to Figure 3. In these averages we have omitted the data from August 23, as suggested in the discussion regarding Table 1. It also should be noted that of the 1° latitude averages from the individual flights that constitute the average in Figure 4, only on September 22 was the aircraft penetration into the ozone hole sufficient to reach a position where the column measurement was less than 200 DU. This occurred from 6° to 8° within the boundary and measured as low as 193 DU. Since TOMS measurements were typically as low as 175 DU in middle to late September, it is clear that virtually all of the ER-2 in situ data were taken
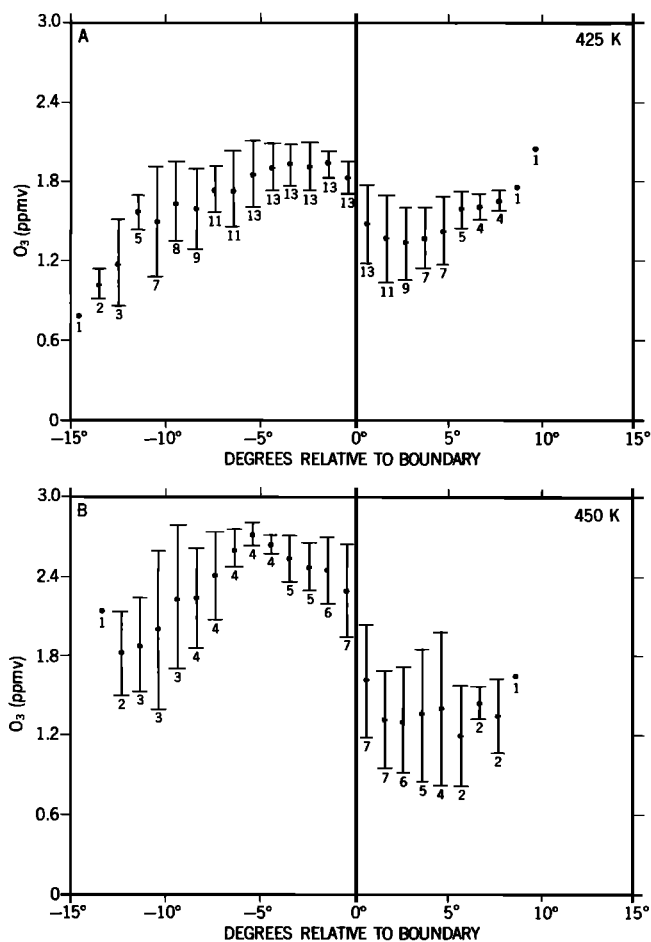
Fig. 3. Plot of averaged ozone versus latitude referenced to the boundary of the chemically perturbed region (vertical line) for (a) the 425 K and (b) the 450 K flight levels. Data are averaged over 1° latitude intervals and over all flights from August 23 through September 22.
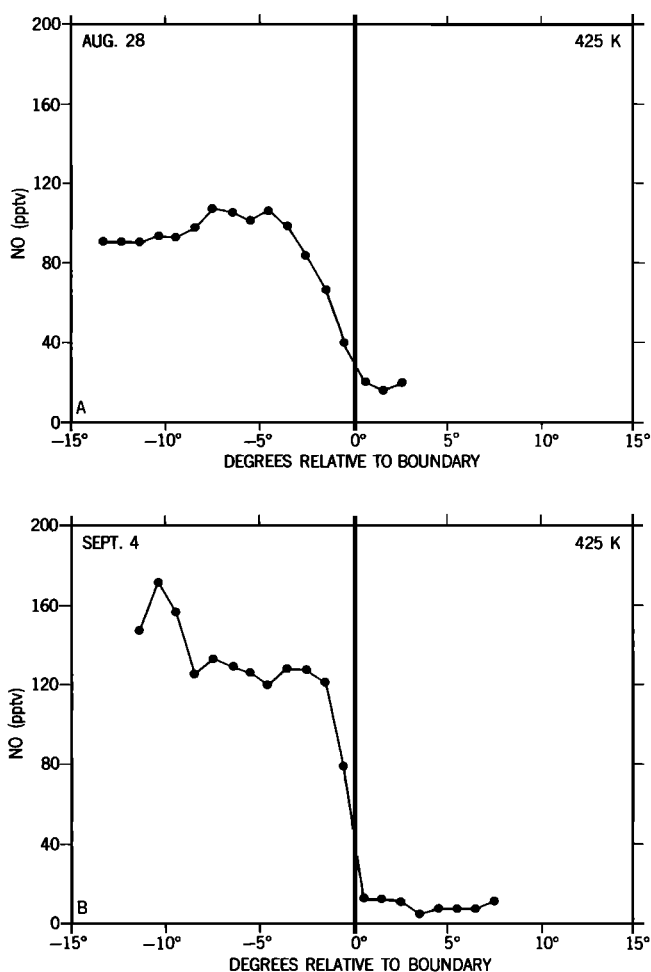

Fig. 5. Plots of NO versus latitude referenced to the boundary of the chemically perturbed region (a) on August 28 and (b) on September 4. Both flights were flown at the 425 K flight level.

outside of the region of largest ozone column loss. If the value of 256 DU is used to represent the value at the boundary (Table 1), we can see from Figure 4 that within the 1σ standard deviation indicated, this value locates the

Fig. 4. Plot of TOMS column ozone measurements along ER-2 flight tracks. Averages were made as in Figure 3, except omitting data from August 23 from the average (see text).

boundary to within about 1° of latitude on the flight dates. This result could be useful for locating the boundary of the ozone hole on days other than the flight dates of the ER-2 and has been used in that fashion by *Toon et al.* [1989].

The NO_y instrument on board the ER-2 was configured to measure NO on two flights [*Fahey et al.* 1989]. The NO flight data are plotted versus latitude for the two flight days, and the boundary is indicated as the heavy vertical line in Figure 5. Again, it is averaged in 1° latitude bins but includes data from southbound and northbound legs. As expected, relatively large values for NO are seen north of the boundary, with the expected low levels to the south. We also note that the decrease in NO begins a few degrees north of the boundary, suggesting a repartitioning of the NO_y species in this region. Figures 6a and 6b show NO_y versus latitude relative to the boundary for the two potential temperature flight levels. In this case, we average over the eight flights on which NO_y was measured, but otherwise the data are averaged as we did for ClO and O_3. Figures 6c and 6d represent an attempt to include only gas-phase NO_y, by selecting the data points for which the corresponding measurement of polar stratospheric cloud particle concentration was low. Since there are no cloud particle data available on September 2, these averages include data only from seven of the 10 flights. The averaged data plots of Figure 6 show
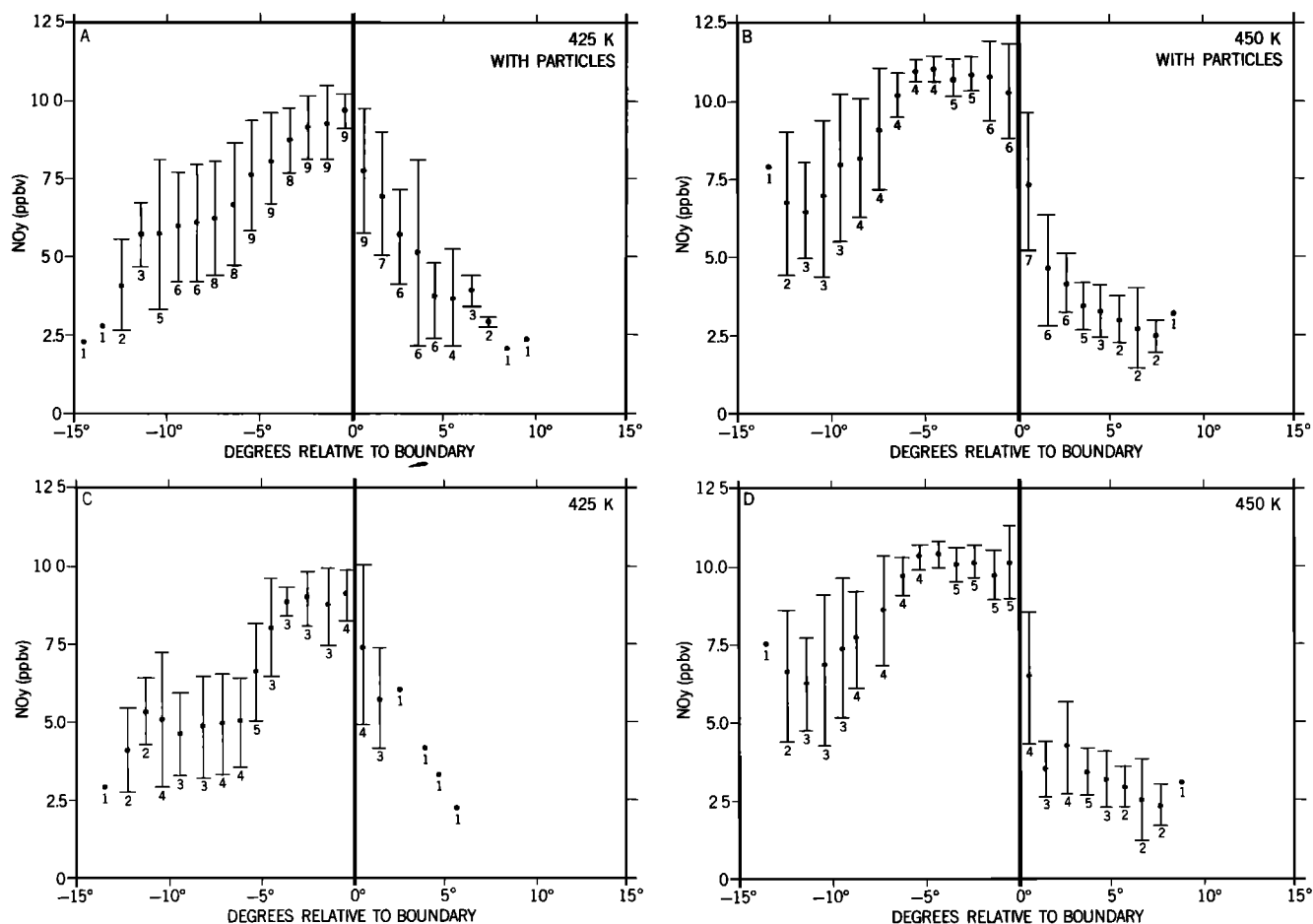
Fig. 6. Plot of averaged NO_y versus latitude referenced to the boundary of the chemically perturbed region (vertical line) for (a) and (c) the 425 K and (b) and (d) the 450 K flight levels. Data are averaged over 1° latitude intervals and in Figures 6a and 6b over all flight legs when NO_y was measured without regard to particulate NO_y. Figures 6c and 6d only include flight data for which the concentration of polar stratospheric cloud particles was low.

either an increase or little change in the first 5° outside the boundary and then an abrupt drop only 1° inside the boundary. These low values provide evidence of denitrification, defined as the large-scale removal of reactive nitrogen species. Denitrification likely results when NO_y species, primarily HNO_3, are incorporated into polar stratospheric cloud particles and grow large enough to sediment out of the stratosphere [Fahey et al., this issue]. As noted earlier, these low NO_y levels are required by the current photochemical models in order to sustain the high ClO levels observed. We have included the temporal trends from the complete NO_y data set (including particles), since there are insufficient data to calculate meaningful trends from the particle-free data set. Therefore caution should be exercised in attaching too much significance to the trend analysis for NO_y in Table 2. The decreases in NO_y at 425 K are consistent with the increase in ClO we previously discussed, but there are insufficient data to do a similar analysis for 450 K.

The measurements of total water (water vapor plus particulate water) on board the ER-2 are described by Kelly et al. [this issue]. Figure 7 shows the averaged data plots for total water, here averaging over all 10 flights. Again, we see a drop from outside to inside at both levels. On the upper level there is also a small poleward decrease indicated in the first 5° outside the boundary, but it is only half of the

decrease seen in crossing the boundary. The low values inside the boundary provide evidence of dehydration, defined as the large-scale removal of water vapor. Some dehydration occurs in the denitrification process, since the particles are primarily composed of water vapor. Additional removal will occur in the absence of condensing NO_y species, when particles of pure water ice are formed and settle out of the stratosphere. The temporal trends in H_2O given in Table 2 show increases over the 1-month period at all positions, except those well within the boundary at 425 K. The increase in H_2O was previously mentioned in the context of the ClO within the boundary. The negative trends at 425 K indicate ongoing dehydration within the boundary during this period.

Nitrous oxide (N_2O) has been discussed relative to the boundary elsewhere in much greater detail than is appropriate here [Proffitt et al., 1989b; Hartmann et al., this issue; Fahey et al., 1989]; however, a few summary remarks are in order. Clearly, the nearly monotonic decrease seen in the averaged data plots (Figure 8) indicates that air of higher stratospheric origin is encountered as we proceed poleward. Indeed, the values indicated within the boundary are characteristic of mid-latitude air, originating at an altitude of about 28 km, with a potential temperature of 700 K. The steepening of the gradient at the boundary indicates some-
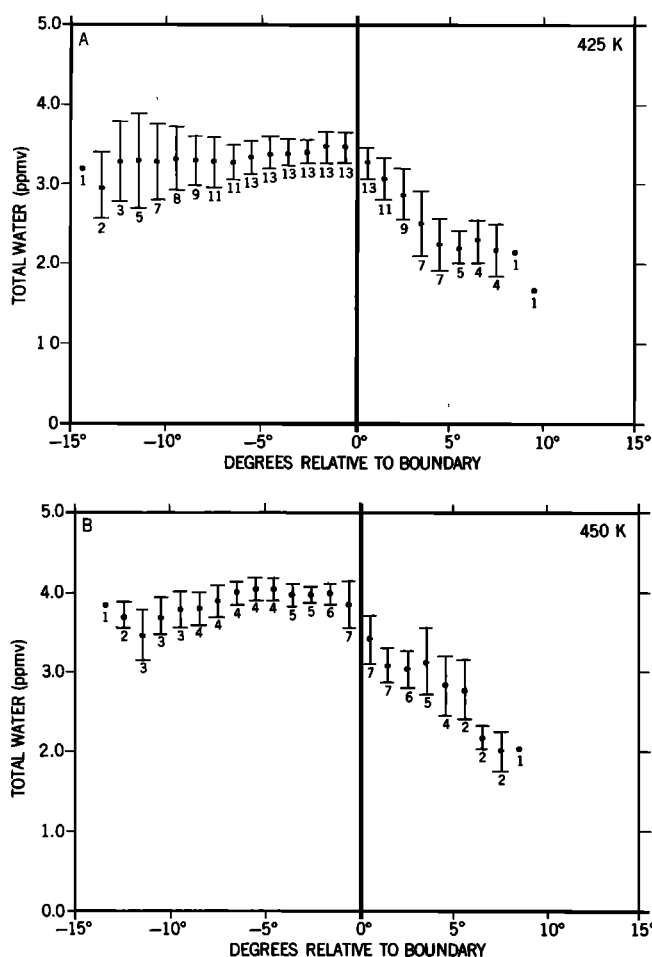
Fig. 7. Plot of averaged total water versus latitude referenced to the boundary of the chemically perturbed region (vertical line) for (a) the 425 K and (b) the 450 K flight levels. Data are averaged over 1° latitude intervals and over all flights from August 23 through September 22.
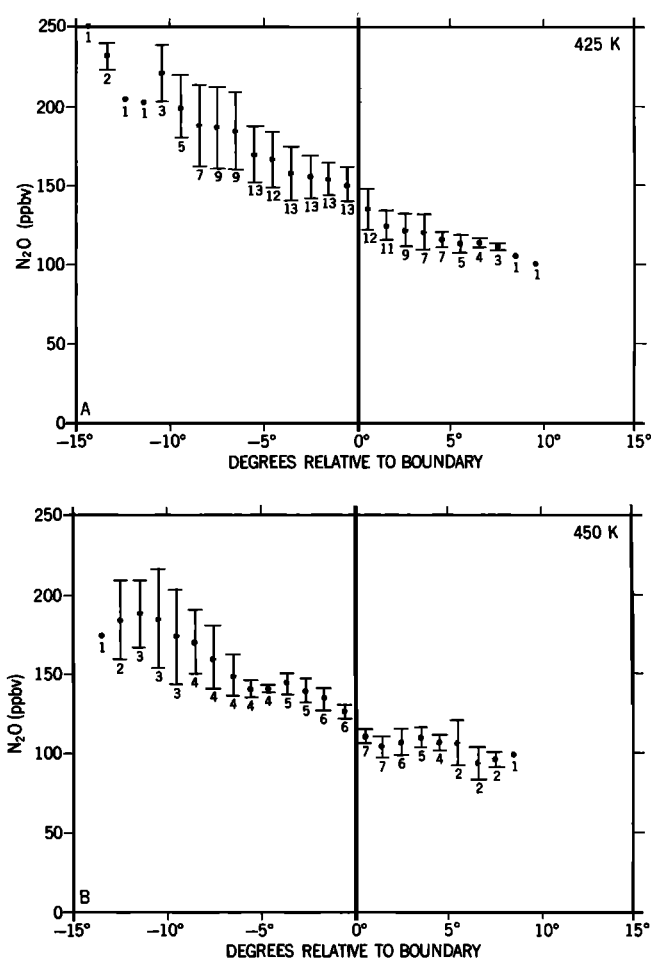
Fig. 8. Plot of averaged nitrous oxide versus latitude referenced to the boundary of the chemically perturbed region (vertical line) for (a) the 425 K and (b) the 450 K flight levels. Data are averaged over 1° latitude intervals and over all flights from August 23 through September 22.

what restricted isentropic transport near the boundary. For, if there were larger-scale isentropic mixing near the boundary, the gradients in N_2O could not be maintained but would be smoothed out. These gradients are maintained by a weak poleward flow and relatively strong diabatic cooling in the presence of the small-scale mixing that is always occurring to some extent. The temporal trends in N_2O (Table 2) are also suggestive of diabatic cooling within the boundary, especially at 425 K, since negative trends indicate that air from above, with its lower values for N_2O, has descended to the lower level during this time period. Details on these arguments can be found in another paper [*Proffitt et al.*, 1989b].

We now consider the meteorological measurements along the ER-2 flight tracks. Since potential vorticity has been shown to be a surrogate for N_2O during the course of the mission [*Schoeberl et al.*, 1989], we will first consider this mathematically derived quantity and later return to the in situ wind, temperature, and potential temperature measurements, thereby easing the transition into the dynamics. (For details on potential vorticity calculations that use only the ER-2 data and the assumptions necessary for the calculations, see *Hartmann et al.* [this issue]. These methods yield results without clear error limits; therefore we have also

included potential vorticity calculated along the ER-2 flight tracks using the National Meteorological Center (NMC) data alone, to compare their results and perhaps increase our confidence in the ER-2 determined calculations. Figure 9 graphically represents the latitudinally averaged data referenced to the boundary. Figures 9a–9d show the potential vorticity increasing (in absolute value) as we approach the boundary from the north, and the values from both analyses compare favorably. But as we proceed across the boundary, the two analyses diverge. The ER-2–derived quantities appear to level off or decrease, while the NMC analysis appears to continue to increase poleward. Although we would expect the NMC analysis to include larger-scale smoothing, the extent of the increase at 450 K in comparison to the ER 2 data and the 10–15% difference in the two analyses at 425 K do not give the authors complete confidence in these calculations inside the boundary. But the similarities in the location of the inflection points of the averaged N_2O plots (Figure 8) and the averaged potential vorticity (ER-2) plots (Figures 9a and 9b) are striking. This increases our confidence in the calculated data. In Table 2 we can compare the temporal trends in potential vorticity (ER-2–calculated only) with the N_2O trends, but only at 425 K. The 450 K potential vorticity data have very large
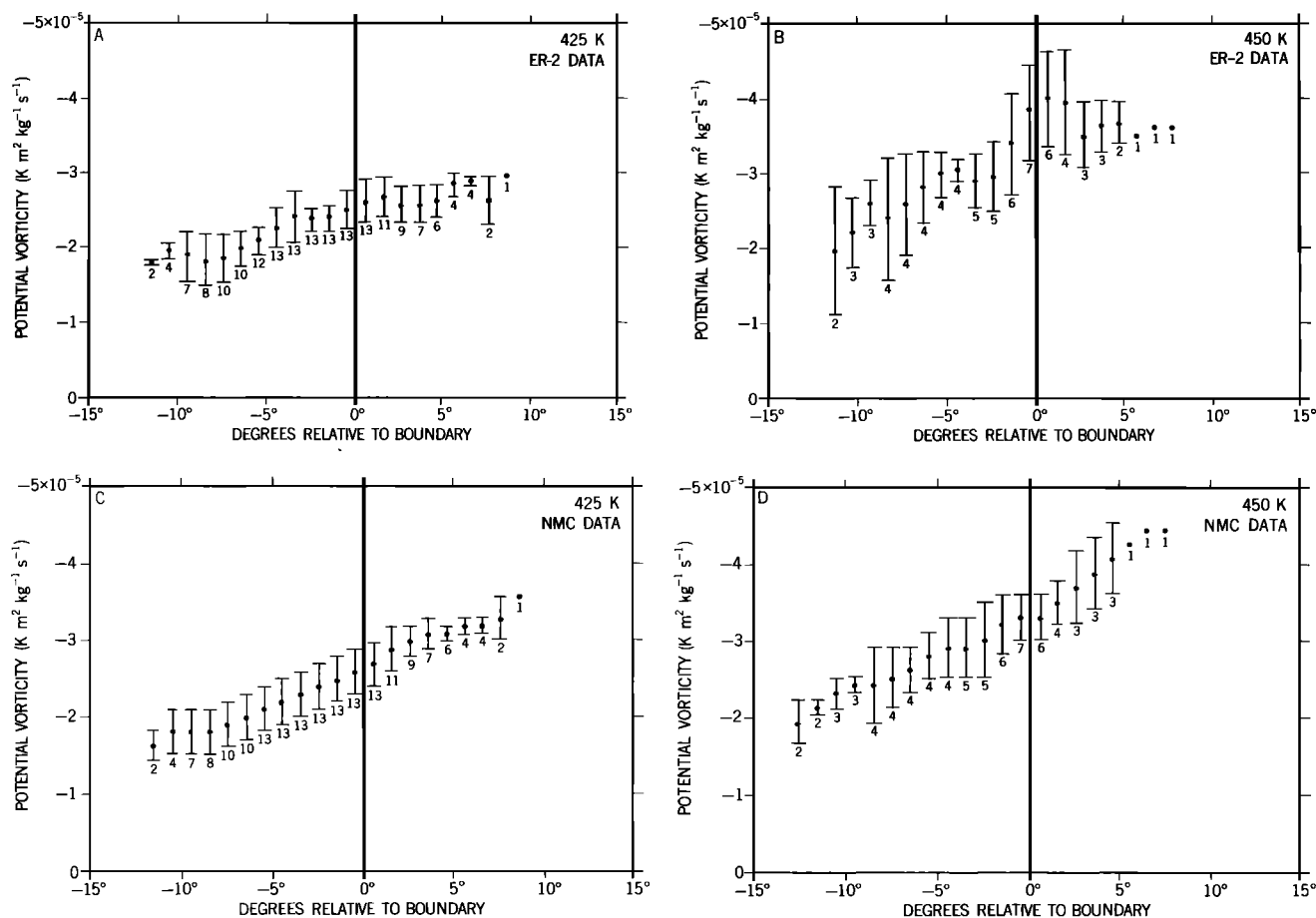
Fig. 9. Plot of averaged potential vorticity versus latitude referenced to the boundary of the chemically perturbed region (vertical line) for (a) and (c) the 425 K and (b) and (d) the 450 K flight levels. Figures 9a and 9b are averages of data calculated from ER-2 flight data alone, while Figures 9c and 9d are from calculations made with NMC data alone. All data are averaged over 1° latitude intervals and over all flights from August 23 through September 22.

standard deviations (Figure 9b) and only a few data points, so the trend analyses yield no results with significant trends, even if the data of August 23 are used in the analysis. However, the trend results at 425 K are generally statistically significant and are in reasonably good agreement with the trends calculated for N_2O inside the boundary. The only place where both have significant nonzero trends but are not consistent is at 5° outside the boundary. We feel that obtaining generally consistent results from two quantities of very different origin suggests that the potential vorticity calculations are dependable, at least for qualitative evaluation. Additionally, since potential vorticity here is a conservative tracer, these analyses lend further credence to the assertion of ongoing poleward diabatic descent of air across the boundary during this period [Proffitt et al., 1989b]. Hartmann et al. [this issue] have proposed that the poleward decreases in N_2O and potential vorticity seen latitudinally are due to the sharp gradient in solar heating associated with the sharp gradient in ozone. However, the poleward decreases in N_2O and potential vorticity were present early in the mission, well before the ozone hole was well developed. Perhaps the temporal trends in potential vorticity and N_2O reflect the temporal trend in the ozone gradient, but it cannot explain the poleward decreases in late August.

Included here, as a meteorological reference, are the averaged data plots for wind speed (Figure 10). The bound-

ary is located south of the peak in the wind speed and in a region where its slope is changing rapidly. On the individual flights that were averaged over 1° intervals, the plot of maximum wind speed relative to the boundary was usually peaked, rather than flat, as in the averaged plot. Of the flight legs with sufficient data to show the peak of the winds, 10 peaked in the first 5° outside of the boundary (one of these peaked on the boundary), and eight peaked from 6° to 12° outside. As an additional indication of the proximity of the boundary to the highest winds, on 13 of the 18 flight legs the winds were at 95% of the wind maximum, within 4° of the boundary. In general, the boundary is located in the region of transition from the high winds to the lower winds in the interior of the vortex, as indicated in the averaged plot. Therefore the boundary of the chemically perturbed region is collocated with a region of high lateral wind shear. Wind shear results in small-scale mixing, which in turn tends to smooth out gradients in trace species. Since strong gradients at the boundary persist throughout the mission, this is further evidence indicating a continuing resupply of unprocessed air from the north and an ongoing dehydration and denitrification of the air as it crosses the boundary going south.

As noted earlier, the temporal trend analysis for wind speed was calculated excluding the data from August 23. The exclusion of August 23 is again due to the abnormal condi-
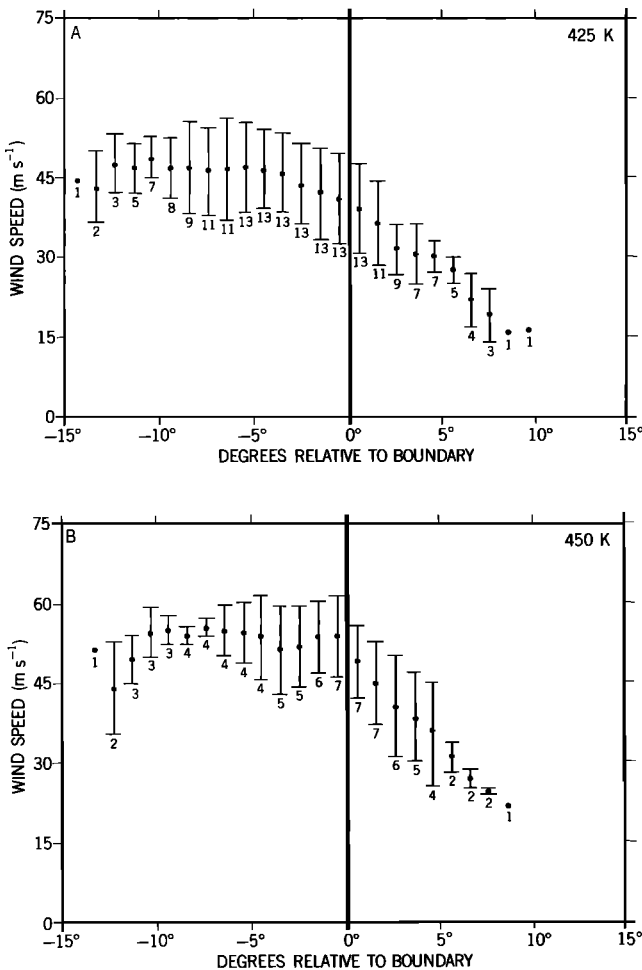
Fig. 10. Plot of averaged wind speed versus latitude referenced to the boundary of the chemically perturbed region (vertical line) for (a) the 425 K and (b) the 450 K flight levels. Data are averaged over 1° latitude intervals and over all flights from August 23 through September 22.
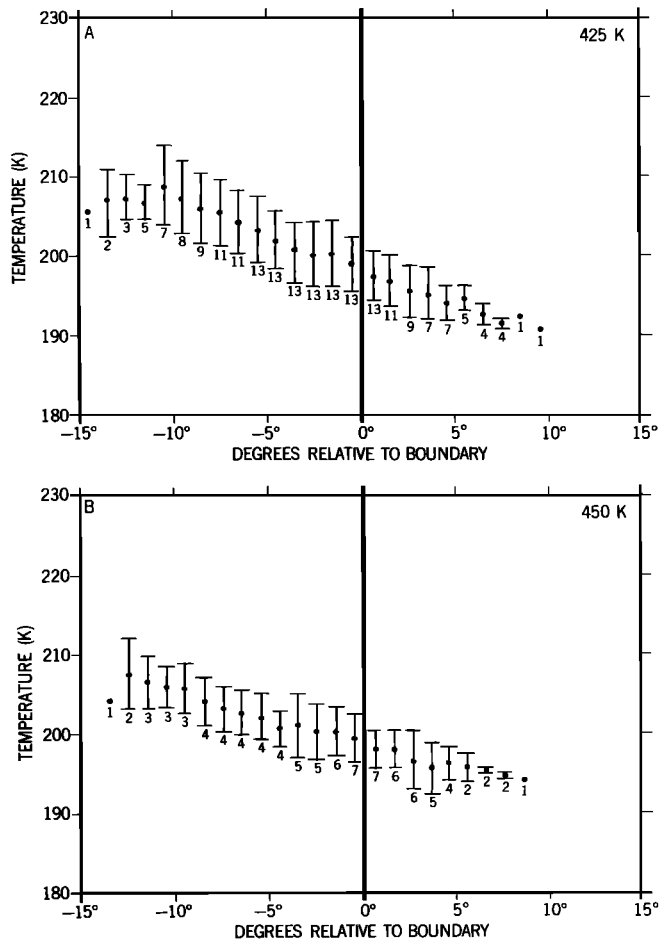

Fig. 11. Plot of averaged temperature versus latitude referenced to the boundary of the chemically perturbed region (vertical line) for (a) the 425 K and (b) the 450 K flight levels. Data are averaged over 1° latitude intervals and over all flights from August 23 through September 22.

tions on that date, when the subtropical jet became coincident with the polar jet, and in this case, increasing the wind speed at flight altitudes to the highest seen over the duration of the mission. On our next flight (August 28) the winds had decreased by 30–40%. The expected temporal increase in the wind speed of the jet can be seen if the August 23 data are excluded; therefore the somewhat restricted analysis seems justified. By excluding these data, the trend analysis at 450 K would begin on September 9, which is too late for meaningful results.

The averaged data plots for temperature are given in Figure 11. Except for the data more than 5° inside the boundary, we see little difference between the two levels. There is the expected decrease in temperature as one proceeds poleward, with an average temperature at the boundary of about 198 K at both levels. The trend analysis is presented only at 425 K, with August 23 data deleted for reasons previously discussed. These trends show an increase in temperature of about 2°–3° outside and 3°–5° inside. The temperature structure and trends are important to consider when analyzing the dehydration and denitrification processes during this period. These considerations are be-

yond the scope of this paper, but they are discussed by *Fahey et al.* [this issue].

Figure 12 and Table 2 present the average potential temperature over the 10 flights. The temporal trends in potential temperature are also given in Table 2. Since the pilots were instructed to fly as close as possible to the prescribed potential temperatures, Figure 12 and Table 2 present measures of the extent of deviation from our goal. Biases both latitudinally and temporally can thus be evaluated. Latitudinally, the lower level has a very gradual increase of about 5 K over about 20° of latitude and has temporal trends of about ±1%. At the upper level the average plot shows a little systematic change outside the boundary but shows a decrease of about 10 K from the boundary to about 5° inside. The temporal trends are also larger at this level. From these analyses we conclude that within the assumed bounds for the flight levels (425 ± 10 K and 450 ± 10 K), there are small systematic changes at 425 K both latitudinally and temporally but that the changes at 450 K are larger and potentially could have a systematic effect on the data. We feel that the ER-2 data set can be further scrutinized and one could extend the analysis given here, but such investigations would require considering
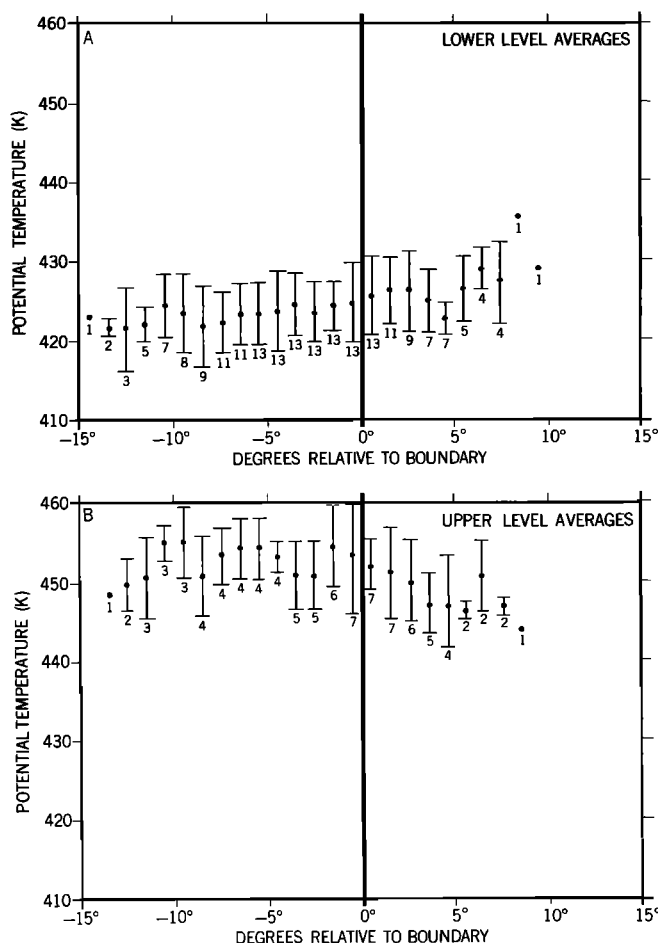
Fig. 12. Plot of averaged potential temperature versus latitude referenced to the boundary of the chemically perturbed region (vertical line) for (a) the lower flight legs (nominal 425 K) and (b) the upper flight levels (nominal 450 K). Data are averaged over 1° latitude intervals and over all flights from August 23 through September 22.

these deviations in potential temperature from the assumed constant potential temperature flight surfaces.

CONCLUSIONS

By defining the boundary of the chemically perturbed region from the ClO level, a narrow transition region (no more than 1° of latitude) is identified that not only separates the very high ClO levels inside from the lower levels outside, but also locates the region of large ozone decrease and separates the highest values of NO, NO_y, and total water from the much lower values within the vortex. The transition zone for the chemically active species (ClO, O_3, NO_y, and NO) extends from about 1° outside to 1° inside the boundary. A somewhat wider transition zone is seen in the other measurements. TOMS total column ozone measurements along the flight tracks of the ER-2 indicate that virtually all of the ER-2 in situ data were taken outside of the region of largest column ozone loss and that a column value of about 260 DU corresponds to the boundary. We do not mean to imply that the chemistry outside of this boundary is not perturbed, nor that all of the ER-2 measurements were made outside the ozone hole. But it does mean that the region outside the boundary is much less perturbed and that this region is not within the ozone hole. Furthermore, from the large temporal decreases of ozone only 1° of latitude inside the boundary, it is clear that the boundary as defined by a level of ClO accurately locates the ozone hole at flight levels.

Interpretations of ClO, H_2O, and N_2O measurements were presented indicating ongoing diabatic cooling and advective poleward transport across the boundary. We have also demonstrated that the boundary is on the poleward side of the Antarctic polar jet and, on the average, located near very high winds and where there is high lateral wind shear. The potential vorticity from ER-2 data at least qualitatively appears to reflect dynamically what the N_2O measurements demonstrate independently. That is, the strong isentropic gradients in N_2O at the boundary indicate restricted isentropic transport, while the potential vorticity calculated from the ER-2, although inherently less accurate and highly smoothed, has a similar character. Clearly, there is a dynamic component that maintains the sharp boundary in ClO by restricting transport at these levels horizontally. However, mixing is always present to some extent, so a resupply of air is also required to maintain the gradient seen in N_2O and potential vorticity. This too is consistent with diabatic cooling and advective poleward transport.

We finally conclude that it is at the boundary that we have the strongest observational evidence linking the large ozone decreases over Antarctica with chlorine chemistry. The precise collocation of the boundary of the ozone hole with the abrupt poleward increases in ClO (along with the consistency of the current chemical mechanisms with the aircraft measurements) strongly implicates man's release of chlorine into the atmosphere as a necessary component in the formation of the Antarctic ozone hole.

REFERENCES

Anderson, J. G., W. H. Brune, and M. H. Proffitt, Ozone destruction by chlorine radicals within the Antarctic vortex: The spatial and temporal evolution of ClO-O_3 anticorrelation based on in situ ER 2 data, *J. Geophys. Res.*, this issue.

Brune, W. H., J. G. Anderson, and K. R. Chan, In situ observations of ClO in the Antarctic: ER-2 aircraft results from 54° to 72°S latitude, *J. Geophys. Res.*, in press, 1989.

Fahey, D. W., D. M. Murphy, K. K. Kelly, M. K. W. Ko, M. H. Proffitt, C. S. Eubank, G. V. Ferry, M. Loewenstein, and K. R. Chan, Measurements of the nitric oxide and total reactive nitrogen in the Antarctic stratosphere: Observations and chemical implications, *J. Geophys. Res.*, in press, 1989.

Fahey, D. W., K. K. Kelly, G. V. Ferry, L. R. Poole, J. C. Wilson,

ID. M. Murphy, M. Loewenstein, and K. R. Chan, In situ measurements of total reactive nitrogen, total water, and aerosol in a polar stratospheric cloud in the Antarctic, *J. Geophys. Res.*, this issue.

Hartmann, D. L., K. R. Chan, B. L. Gary, M. R. Schoeberl, P. A. Newman, R. L. Martin, M. Loewenstein, J. R. Podolske, and S. E. Strahan, Potential vorticity and mixing in the south polar vortex during spring, *J. Geophys. Res.*, this issue.

Hofmann, D. J., J. W. Harder, S. R. Rolf, and J. R. Rosen, Balloon-borne observations of the development and vertical structure of the Antarctic ozone hole in 1986, *Nature*, *326*, 59–62, 1987.

Kelly, K. K., et al., Dehydration in the lower Antarctic stratosphere during late winter and early spring, 1987, *J. Geophys. Res.*, this issue.

Ko, M. K. W., J. M. Rodriguez, N.-D. Sze, M. H. Proffitt, W. L. Starr, A. J. Krueger, E. V. Browell, and M. P. McCormick, Implications of AAOE observations for proposed chemical explanations of the seasonal and interannual behavior of Antarctic ozone, *J. Geophys. Res.*, in press, 1989.

Krueger, A. J., P. E. Ardanuy, F. S. Sechrist, L. M. Penn, D. E. Larko, S. D. Doiron, and R. N. Galimore, The 1987 Airborne Antarctic Ozone Experiment: The Nimbus 7 TOMS data atlas, *NASA Ref. Publ., NASA RF-1201*, Goddard Space Flight Center, Greenbelt, Md., March 1988.

McElroy, M. B., R. J. Salowitch, S. C. Wofsy, and J. A. Logan, Reductions of Antarctic ozone due to synergistic interactions of chlorine and bromine, *Nature*, *321*, 759–762, 1986.

Molina, L. T., and M. J. Molina, Production of Cl_2O_2 from the self-reaction of the ClO radical, *J. Phys. Chem.*, *91*, 433–436, 1987.

Murphy, D. M., A. F. Tuck, K. K. Kelly, K. R. Chan, M. Loewenstein, J. R. Podolske, M. H. Proffitt, and S. E. Strahan, Indicators of transport and vertical motion from correlations between in situ measurements in the Airborne Antarctic Ozone Experiment, *J. Geophys. Res.*, this issue.

Proffitt, M. H., et al., In situ measurements within the 1987 Antarctic ozone hole from a high-altitude ER-2 aircraft, *J. Geophys. Res.*, in press, 1989a.

Proffitt, M. H., K. K. Kelly, J. A. Powell, B. L. Gary, M. Loewenstein, J. R. Podolske, S. E. Strahan and K. R. Chan, Evidence for diabatic cooling and poleward transport within and around the 1987 Antarctic ozone hole, *J. Geophys. Res.*, in press, 1989b.

Rodriguez, J. M., et al., Nitrogen and chlorine species in the spring Antarctic stratosphere: Comparison of models with AAOE observations, *J. Geophys. Res.*, in press, 1989.

Schoeberl, M. R., et al., Reconstruction of the constituent distribution and trends in the Antarctic polar vortex from ER-2 flight observations, *J. Geophys. Res.*, in press, 1989.

Solomon, S., R. R. Garcia, F. S. Rowland, and D. J. Wuebbles, On the depletion of Antarctic ozone, *Nature*, *321*, 755–757, 1986.

Toon, G. C., C. B. Farmer, L. L. Lowes, P. W. Schaper, J.-F. Blavier, and R. H. Norton, Infrared aircraft measurements of stratospheric composition over Antarctica during September 1987, *J. Geophys. Res.*, in press, 1989.

Tuck, A. F., Synoptic and chemical evolution of the Antarctic vortex in late winter and early spring, 1987, *J. Geophys. Res.*, this issue.

Tuck, A. F., R. T. Watson, E. P. Condon, J. J. Margitan, and O. B. Toon, The planning and execution of ER-2 and DC-8 aircraft flights over Antarctica, August and September 1987, *J. Geophys. Res.*, this issue.

K. R. Chan, M. Loewenstein, and J. R. Podolske, Mail Stop 245-5, NASA Ames Research Center, Moffett Field, CA 94035.

D. W. Fahey, K. K. Kelly, J. A. Powell, M. H. Proffitt, and A. F. Tuck, Aeronomy Laboratory, ERL, NOAA, 325 Broadway, Boulder, CO 80303.

B. L. Gary and J. J. Margitan, Jet Propulsion Laboratory, California Institute of Technology, Pasadena, CA 91109.

A. J. Krueger and M. R. Schoeberl, Mail Stop 616, NASA Goddard Space Flight Center, Greenbelt, MD 20771.